

Study the effect of adding Oleic acid to reduce the medium diffusion in pores of hybrid silica-based sol-gel coatings

MUSSA, Magdi, TAKITA, Sarra, ZAHOOR, Deeba, LEWIS, Oliver and FARMILO, Nick <<http://orcid.org/0000-0001-5311-590X>>

Available from Sheffield Hallam University Research Archive (SHURA) at:

<http://shura.shu.ac.uk/29505/>

This document is the author deposited version. You are advised to consult the publisher's version if you wish to cite from it.

Published version

MUSSA, Magdi, TAKITA, Sarra, ZAHOOR, Deeba, LEWIS, Oliver and FARMILO, Nick (2021). Study the effect of adding Oleic acid to reduce the medium diffusion in pores of hybrid silica-based sol-gel coatings. In: The 2nd International Online Conference on Polymer Science - Polymers and Nanotechnology for Industry 4.0, Basel, Switzerland, 1-15 Nov 2021. sciforum-MDPI.

Copyright and re-use policy

See <http://shura.shu.ac.uk/information.html>

Study the effect of adding Oleic acid to reduce the medium diffusion in pores of hybrid silica-based sol-gel coatings [†]

Magdi Hassn Mussa ^{1,2,3,*}, Sarra Takita ⁴, Farah Deebe Zahoor ^{4,5}, Oliver Lewis ⁴, Nicholas Farmilo ^{4,6}

¹ Mechanical and Energy Department, The Libyan Academy of Graduate study, Tripoli, Libya

² Mechanical Engineering Department, Sok Alkhamis Imsehel High Tec. Institute, Tripoli, Libya

³ The Institute of Marine Engineering, Science and Technology, London, UK; magdimosa1976@gmail.com (MM)

⁴ Materials and engineering Research institute MERI, Sheffield Hallam University, Howard Street, Sheffield, UK ; Sarah.a.talita@gmail.com (ST), O.Lewis@shu.ac.uk (OL)

⁵ Department of Chemistry, University of Sheffield, Sheffield, UK ; F.Zahoor@sheffield.ac.uk (DF)

⁶ Tideswell Business Development Ltd, Ravensfield Sherwood Rd, Buxton, UK ; nfarmilo@gmail.com (NF)

* Correspondence: magdimosa1976@gmail.com; Tel.: +447404496955

[†] Presented at the 2nd International Online Conference on Polymer Science - Polymers and Nanotechnology for Industry 4.0- in Session of Smart polymeric Synthesis and Modification for Industry 4.0at 15–30 Nov 2021

Abstract: Due to the wide-ranging of preservative surfaces applications, there is a need for a fundamental understanding of not only how to produce such exceptional surfaces but also to know how specific surface properties affect coatings pore wettability, for example, morphology and chemical comprehending. Silica-based hybrid coatings as advanced hybrid polymers have been shown to exhibit excellent chemical stability with a chance to be functionalised combined with reducing the corrosion of metal substrates. However, research shows that sol-gel only has some limitations in terms of anti-corrosive properties due to the high porosity. Therefore, this work will report the preliminary performance of the diffusion prevention in a silica-based hybrid sol-gel coating that has been enhanced by adding Oleic acid (OA) to the sol-gel formula. The evaluation of the effect of the adsorption mechanism of OA on aluminium alloys surface was studied based upon using infrared analysis (FTIR) as a non-destructive test separately. The chemical confirmation of adding OA to Sol-gel was done by infrared spectroscopy (ATR-FTIR) and supported by analysing the morphology of the surface by using scanning electron microscopy (SEM) and water contact angle test (WCA). Furthermore, the coatings' corrosion performances were studied using electrochemical impedance spectroscopy (EIS) and Potential-dynamic polarisation scanning (PDPS). As a result, the Oleic acid - silica-based hybrid coating exhibited exceptional functionalised pore-blocking, hydrophobic and anti-corrosion properties, providing mimicked active protection on the aluminium alloy 2024-T3 samples compared to sol-gel-only and non-coated samples.

Keywords: Silica-based hybrid sol-gel coating, infrared spectroscopy, electrochemical testing, corrosion protection

Citation: Mussa, M.H.; Takita, S.; Deebe, F.Z.; Lewis, O.; Farmilo, N.: Study the effect of adding Oleic acid to reduce the medium diffusion in pores of hybrid silica-based sol-gel coatings. *Mater. Proc.* **2021**, *3*, x. <https://doi.org/10.3390/xxxxx>

Published: date

Publisher's Note: MDPI stays neutral with regard to jurisdictional claims in published maps and institutional affiliations.



Copyright: © 2021 by the authors. Submitted for possible open access publication under the terms and conditions of the Creative Commons Attribution (CC BY) license (<https://creativecommons.org/licenses/by/4.0/>).

1. Introduction

There are potentially numerous applications in industries involving sol-gel derived technologies. The sol-gel processes can produce a variety of different materials, including coatings, films, fibres, monoliths, and nanosized powders. Coatings or thin films produced by the sol-gel technology are the typical representatives in the early commercial involvement. Spinning, spraying, dipping and spreading methods can be used to create thin films without forming any cracks. Other examples of coating applications of the sol-gel films include self-cleaning coatings, hydrophobic or hydrophilic coatings, and anti-

corrosion and wear-resistance coatings[1–4]. Sol-gels are considered an excellent alternative to replace conventional treatments, many of which are almost to be banned in some world regions, such as chromate conversion coatings. Sol-gel advantages come via the low initial cost and effectiveness of this coating. Spatially it is considered as an eco-friendly coating comparing to the other alternative surface treatments. Also, the advantages of sol-gel over the conventional coating methods are the ease of preparation. Controlled crack-free films can also ease deposit a wide range of inorganic oxide in the matrix at a lower temperature [5,6].

Aluminium alloys, especially AA2024-T3, are widely used in aerospace and structural industries because of their high specific strength ratio. Due to this, the element of copper in these alloys is used to improve its mechanical stiffness. However, this, in turn, can result in microscopic galvanic couples, which increase the potential for corrosion on these alloys. To avoiding localised corrosion that could damage the mechanical properties of structures, the general practice is to prevent the direct interaction of the electrochemically active matrix with the environment by applying a protective coating system with the intention of prolonging the service life of parts before applying a painting application. The alloy is frequently clad or anodised to provide good bonding between the paint and the substrate[7,8].

Oleic acid was one of the recommended fatty acids mentioned previously in a US Army report from 1991 for use as a corrosion inhibitor in engines [9]. Oleic acid is created in nature in various animal lards and vegetable fats and oils with the chemical structure of $C_8H_{17}CH=CH(CH_2)_7COOH$ [10]. It is pH neutral and colourless in its appearance, though commercially produced material may be yellowish in colour. It is an unsaturated fatty acid with non-polar properties. The chemical structure can be seen in figure 1.

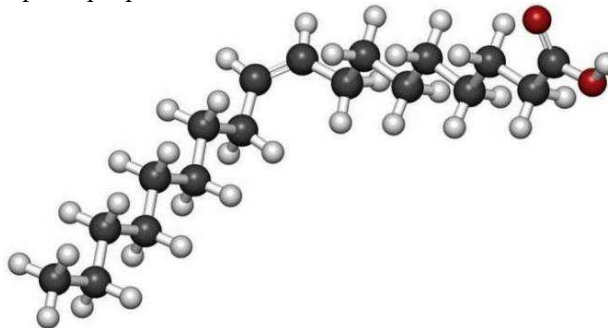


Figure 1, the chemical structure of Oleic acid [11]

Malik M. A. et al. and Migahed A. et al. [12,13] mentioned in their publications that the mechanism of inhibition is complicated and depends on many factors, including the creation of mono/multidimensional protecting layers on the metal surface. As well as the other factors that work with the protective layers are the interactions between inhibitors and substrate, chemical reactions that could occur, electro-potentials effects, operational temperatures, the concentration of the inhibitor and finally the properties of the treated surface.

Also, in another technique by Zhang. W et al. [14] as mentioned, it can be made water-soluble by the synthesis in polyethene glycol and imidazole to use as an injectable inhibitor in aquatic media.

There is some limitation of direct use of the fatty acids with other coatings, including Sol-gel, which decreases the cross-links in the coating matrix and will prevent creating a coating with good adhesion on the substrates due to increasing the hydrophobicity on top of the metal surface. In his review, Hughes A. et al. [11] mentioned the encapsulation of $La(dibutyl\ phosphate)_3$ with micelle oleic acid in epoxy coatings were investigated. In fact, there has been mention of the use of oleic acid in some patents to be used in conjunction

with other inhibitors. Simendinger W. et al. [15] mentioned in his patent the use of oleic acid with other material in sol-gel as an antifouling release agent.

Although the previous studies presented functional corrosion inhibition of oleic acid on steel alloys, the term of use oleic acid as corrosion inhibitor encapsulated in sol-gel was not mentioned so far on published work or patents. Therefore, as a research gap, this part will be investigated and try to be covered in this paper.

2. EXPERIMENTAL WORK

2.1. Sol-Gel preparation

In this study, the used hybrid silica-based sol-gel was synthesised from tetraethyl orthosilicate silane (TEOS) and trimethoxymethyl silane (MTMS) purchased from Sigma-Aldrich. As mentioned in the previous work, the silica-based sol-gel mixture was then enhanced by adding poly-siloxane (PSES) solution [1]. This formula was used as the baseline coating and labelled SHX-80. The oleic acid (OA) modified hybrid silica-based sol-gel is labelled as OA-SHX-80. It was prepared by encapsulating 0.1 to 0.3 vol.% of solution 1:1 of ethanol and oleic acid (OA) purchased from Sigma-Aldrich into the original SHX-80 by wise dropping and stirring. The formulation was then left for 24 hours stirring to complete its hydrolysing and condensation.

2.2 Substrate Preparation and Film Deposition

The aluminium alloy AA2024-T3 Q-panels made with dimensions of (102 mm × 25 mm × 1.6 mm) were purchased from Q-Lab for use as test substrates [16]. First, the received Q-panels were washed with a commercial aluminium base surfactant cleaner and then rinsed with DI water, then rewashed with acetone to remove organic residues on the surface. Then spray the sol-gel to the pre-cleaned aluminium alloy substrates. The distance from the spraying gun to the surface was approximately 150 mm. Over three passes, the coating was built up to keep the thickness standard for all samples about 15 μm ±2. After that, the coated samples were left in the air for 10 min before being annealed at 80° C for 4 hours. Table 1 shows experiment codes used to identify the coated samples.

Table 1. sample identification table

No.	Identifier	Formula Base Composite	(OA)	Curing Temperature
1-	SHX-80	TEOS+MTMS+PSX	-	80°C
2-	OA-SHX-80	TEOS+MTMS+PSX	yes	80°C
3-	Bare AA2024 T3	-	-	-

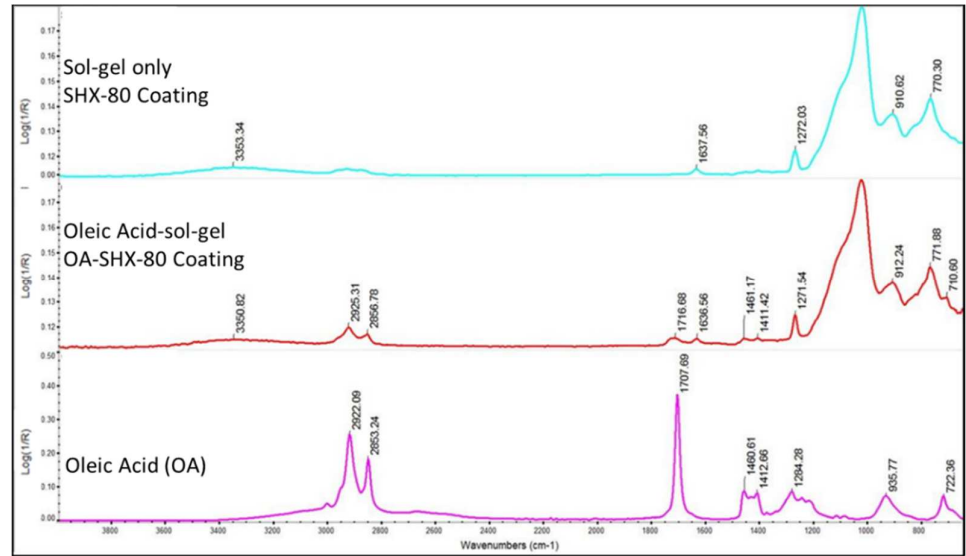
3. Results and discussion

3.1 ATR-FTIR for OA-SBX-80 sol-gel chemical composition

The organic OA was successfully incorporated into the SHX sol-gel by comparing the infrared spectrum obtained from the OA-SHX-80 coating to the unmodified SHX-80. This is enlarged in figure 2. The FTIR spectrum confirms that the organic-inorganic hybrid sol-gel coating of OA-SBX-80 and HXS-80 was well attached to the AA2024-T3 substrate. Also, the chemical composition can be seen for the SBX-80 sol-gel formula and the oleic acid modified coating.

The spectrum obtained from the OA-SBX-80 sol-gel formula has broad fingerprint peaks similar to the basic formula SBX sol-gel. However, the successful incorporation of adding oleic acid (OA) into the base formula of SBX-80 sol-gel was confirmed by comparing the infrared spectrum obtained from the OA-SBX-80 coating to the unmodified SBX-80. The alkyl group presents two main contributions at 2925 cm⁻¹ and 2856 cm⁻¹, representing CH₃ and CH₂ stretching, respectively. Additional peaks are characteristic of the confirmation of CH₂ at 1460 cm⁻¹ and 1300 cm⁻¹. As expected, the carbonyl function, C=O is shown by a peak at 1707 cm⁻¹ [17–19].

1



2

Figure 2, ART-FTIR spectra show the effect of OA adding to the SHX-80 sol-gel.

3

3.2 Understand the adsorption mechanism of OA on aluminium alloys surface

4

This mechanism could be summarised in the following sequence: firstly, the fatty acid acts as surfactant inhibitors in the surrounded aggressive environment and then is adsorption of surfactant molecules on top of the metallic surface by creating a metallic binding. This process is usually affected by surface charges, the surfactant’s chemical structure, and the surrounding electrolyte. Consequently, the adsorption will occur due to the interaction potential between the surfactant and metal surface, and as a result, the inhibiting effect of the molecules is credited to its functional groups that attach to surfactants on the metallic surface. There are three individual types of adsorption coordination that the carboxylate group in fatty acid can adopt for bonding to the metallic surface: proposed structures of the mono-dentate, bidentate, and bridging coordination types shown in Figure 3. In the bridge-bonded configuration, the oxygen atoms are identical but on different aluminium atoms, while on the other bonding will be connected to one metallic atom [20]. Besides, the rate of adsorption is usually rapid, and henceforth the weak metallic alloy surface will be shielded well and protected from direct contact with the aggressive media. [12,13]

5

6

7

8

9

10

11

12

13

14

15

16

17

18

19

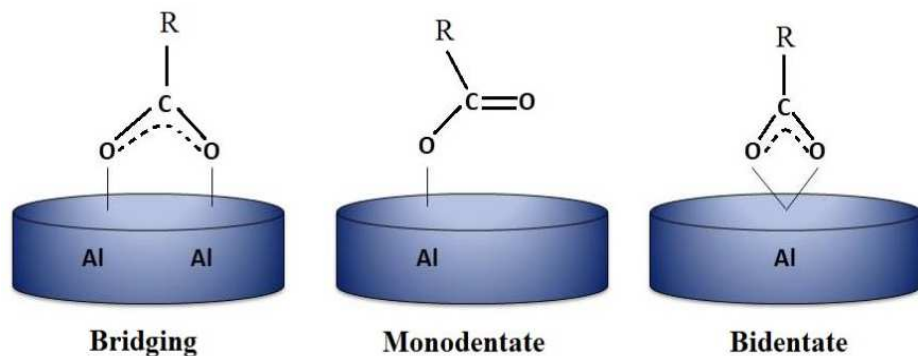


Figure 3, Schematic representations for three types binding adsorption process of carboxylate groups in fatty acid on steel aluminium surface [71]

20

21

22

3.3 Water Contact Angle of SBX And OA-SBX Coatings

In figure 4, the results of the measured water contact angle (WCA) show the original SHX-80 coating were measured about $67^\circ \pm 2$, and as shown in (a), and the measured WCA on modified OA-SHX-80 Sol-gel coating was $102^\circ \pm 4$, and as shown in (b), as the higher water contact angle recorded for the OA-SHX-80 shows that its wettability is lower than that of the original SHX-80 [21].

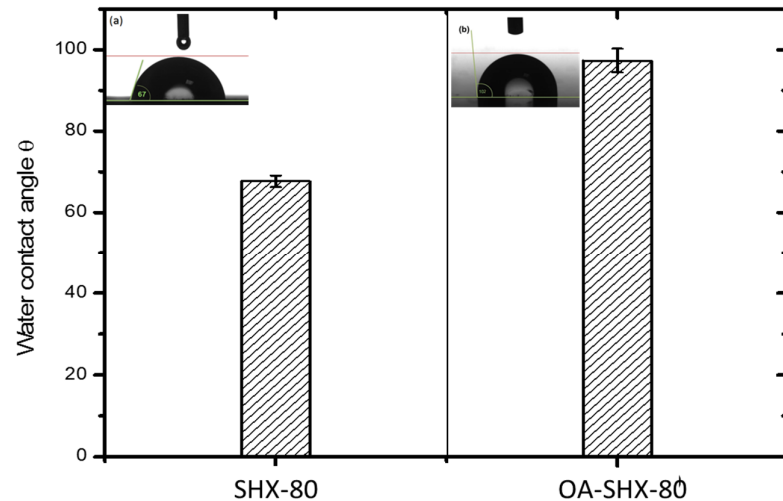


Figure 4. Bar chart showing mean values of WCA of OA-SHX-80 and SHX-80 coatings, Optical images showing water droplets on (a) SHX-80 and (b) modified OA-SHX-80 coatings

3.4 Potentiodynamic polarisation scanning (PDPS)

All coated samples displayed remarkable performance properties compared to the bare AA2024 sample. The corrosion potential (E_{corr}) and corrosion current density (I_{corr}) were obtained from the shown in figure 5. the current density on the cathodic branch of the Tafel curve for all coated samples is reduced by more than three magnitudes when compared to the bare AA2024-T3. Nevertheless, the 0.1 % v/v oleic acid sol-gel OA-SHX-80 coated sample comes the lowest, as it was reduced by seven orders of magnitude to bare AA2024-T3. This is attributed to the surface-active molecule and diffusion prevention of oleic acid. However, 0.3% v/v oleic acid sol-gel OA-SHX-80 coated sample shows the same pattern except it collapsed showed less protection on the anodic branch, reveals the failure in protection in the potential of -502 mV due to the initiate of pitting and coating failure. The SHX-80 sol-gel only showed a reduction in the anodic branch by about four and a half orders of magnitude less than the bare AA2024-T3.

The information that obtained of Corrosion current densities of bare and coated samples were reduced to $2.88 \times 10^{-9} \text{A/cm}^2$ for (0.1 OA-SHX-80), $3.02 \times 10^{-9} \text{A/cm}^2$ for (0.3 OA-SHX-80) and $6.41 \times 10^{-9} \text{A/cm}^2$ for (SHX-80) respectively, and as compared to $6.8 \times 10^{-6} \text{A/cm}^2$ of the bare AA2024-T3 alloy. The shift in E_{corr} indicates that the anodic is inhibited to a greater degree than the cathode in 0.1 and 0.3 OA-SHX 80 sol-gel mixture. This could be attributed to oleic acid pores-blocking by increasing the hydrophobicity in the filled pores, which reduces the electrolyte diffusion to the surface of the metallic substrate [12,13].

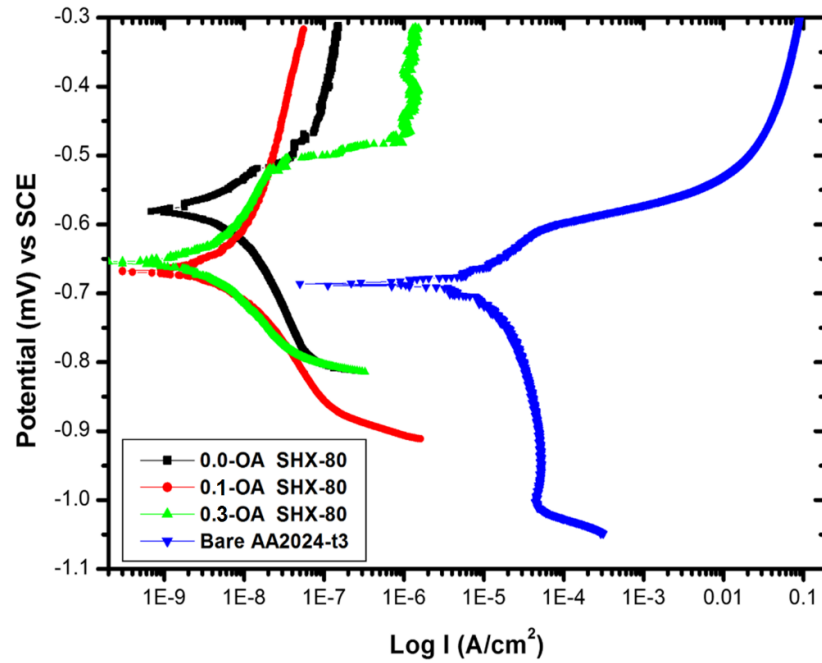


Figure 5, (PDPs) Polarization curves for the bare and sol-gel coated samples with different concentrations of OA organic inhibitors in 3.5% NaCl

3.4 Electrochemical Impedance Spectroscopy (EIS)

3.4.1 Impedance magnitude Bode plots

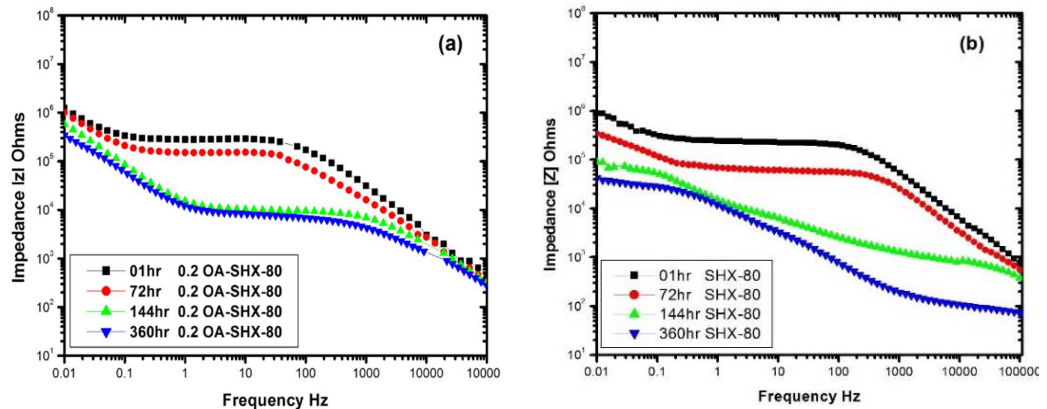


Figure 6, Impedance magnitude for (a) OA-SHX-80 and (b) SHX-80.

This test will continue with 0.1 % OA-sol-gel coating as it not affecting the sol-gel matrix. As it is shown in figure 6, after the first hour of immersion, the overall impedance of OA-SHX-80 at low frequencies was started by approximately in the same magnitude to SHX-80 coated samples, with values of 1.1×10^6 ohms.cm⁻² (OA-SHX-80), compared to 9.8×10^5 ohms.cm⁻² (SHX-80). After 360 hours, the OA-SHX-80 coated samples dropped about one and a half orders of magnitude; this could be due to the electrolyte diffusion and expansion of the pores in the coating matrix. However, this drop does not affect the electrolyte's generally visible protection, suggesting the film of OA has been created on the metal surface [10]. A noticeable measured impedance was observed to the SHX-80 coated sample at about 3.5×10^4 ohms.cm⁻² after 360 hours compared to OA sol-gel at about 2.5×10^5 ohms.cm⁻². This might be attributable to the coating resistance beginning to reduce due to the creation of rounded pitting under the coatings. Also, the high frequencies impedance falls of about one of magnitude; this impedance is considered higher than SBX-

80 coating in the middle-frequency range between 10^5 to 10^6 Hz. It may be attributed to the coating pores and cracking that occurred.

3.5 Using Nyquist plots for Investigating the corrosion protection behaviour

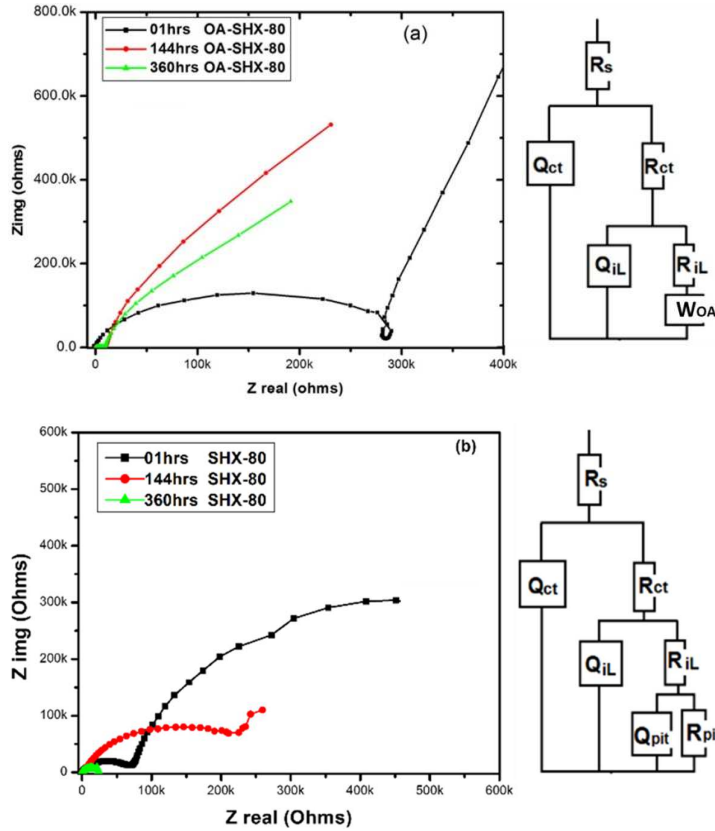


Figure 7, showing the Nyquist plot for (a) OA-SHX-80 and (b) SHX-80 coating systems, with a schematic drawing of system behaviour simulation (a) OA-SHX-80 and (b) SHX-80 after 144 hr of immersion in 3.5% NaCl solution

The Nyquist plots for figure 7 (a) OA-SHX-80 and (b) SHX-80 coatings from 01 to 360 hr, respectively. These plots were used to obtain the equivalent circuits modelling fitting using ZSimpwin electrochemical impedance spectroscopy (EIS) data analysis software.

Tables 2 and 3 below demonstrate the fitted data for the SHX-80 and the OA-SHX-80 coatings after various immersion times. The equivalent circuits were used to simulate the corrosion reaction on the surface of coated samples in 01 hr, 48hrs and 144 hrs, respectively. Instead of using an ideal capacitor (C), a time-constant element (Q) was used to companies the current leakage in the capacitor and/or frequency dispersion effect of the alternating current signals [22]. The suggested equivalent circuits for each of the EIS plots after 144hrs were provided in the figure for both systems.

The elements samples identifier used for the equivalent circuits were: solution resistance (R_s), coating resistance (R_{ct}), coating constant phase elements (Q_{ct}), interfacial layer resistance (R_{iL}), interfacial layer capacitance (Q_{iL}), oxide layer (pitting) resistance (R_p), oxide layer (pitting) capacitance (Q_p) and Warburg-circuit element (W) [23]

Table 2 The fitted data obtained from EIS spectra for the OA-SHX-80 sol-gel coating after various immersion times in 3.5 wt. % NaCl solution.

Circuit	Element	Immersion time(hrs)		
		01	48	144
		R(Q(R(Q(RW))))	R(Q(R(Q(RW))))	R(Q(R(Q(RW))))
	R _s	102	205	195
	Q _{ct}	1.089E-8	2.155E-8	1.044E-7
	n	0.9138	0.888	0.772
	R _{ct}	2.878E5	1.232E4	8.770E3
	Q _{il}	9.956E-6	1.577E-5	2.026E-5
	n	0.9296	0.897	0.916
	R _{il}	1.667E6	5.688E6	8.594E5
	W _{oA}	4.554E-7	1.041E-6	6.716E-6

Table 3 The fitted data obtained from EIS spectra for the SHX-80 sol-gel coating after various immersion times in 3.5 wt. % NaCl solution.

Circuit	Element	Immersion time(hrs)		
		01	48	144
		R(Q(R(QR)))	R(Q(R(Q(R(QR))))	R(Q(R(Q(R(QR))))
	R _s	100	205	225
	Q _{ct}	1.079E-7	2.850E-7	4.771E-6
	n	0.800	0.627	0.490
	R _{ct}	7.287E4	815	253
	Q _{il}	4.933E-6	1.151E-6	3.912E-6
	n	0.850	0.694	0.896
	R _{il}	7.793E5	4.022E5	1.221E5
	Q _p	-	7.364E-5	4.835E-5
	n	-	0.900	0.455
	R _p	-	1.369E6	1E20

3.6 Scanning Electron microscopy images after immersion

Figure 8 shows the surface morphology of the three samples, OA-SHX-80 and SHX-80. As showed in figure 8 (b), the SHX-80 exhibited was susceptible to the development of microcracks when dried in open atmospheric conditions after long immersion. The cracks were observed around 1-6 μm wide on the surface of the coating, with some pitting under the coating. Exposure to the aluminium alloy substrate due to coating cracking can poorly affect the provided barrier corrosion protection, which has implications for wet/dry cycling is experienced. The OA-SBX-80 coating showed excellent resistance to corrosion and cracks under similar circumstances, in figure 8 (a) showed that the OA-SHX-80 was more stable than the SHX-80, which may be attributed prevent the diffusion in the coating system, in line with the self-healing inhibition properties of OA.

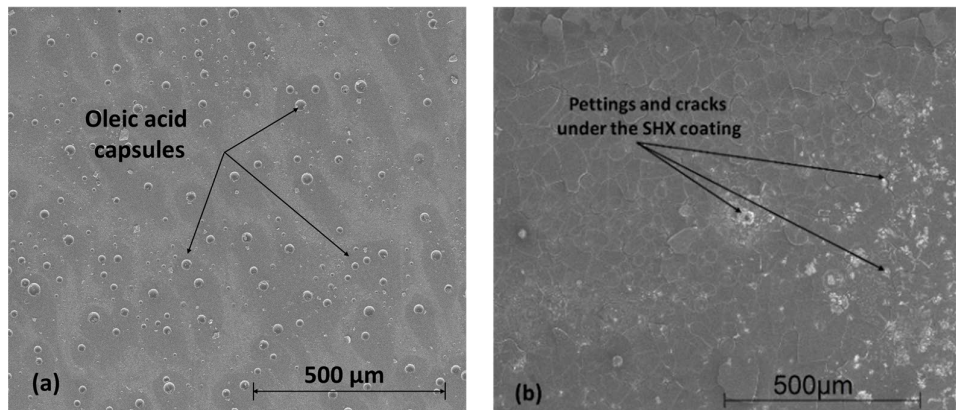


Figure 8, SEM surface images for (a) OA-SHX-80 coating, (b) SHX-80 coating after 360hrs of immersion

4. Conclusion

As a corrosion coating, the silicate-based hybrid SHX Sol-gel formula can provide good barrier protection without the presence of any inhibitor. However, The protection can last for at least a maximum of ten days in 3.5% NaCl solution before cracks and pitting can be appeared visually on the surface. By encapsulating the oleic acid in the silica-based sol-gel, it revealed improved corrosion protection when combined with the base sol-gel coatings. 0.1% oleic acid-enhanced coating can provide protection over two weeks in an aggressive simulated environment of 3.5% NaCl without any failure sign. Adding oleic acid as an inhibitor to the sol-gel matrix provides mimicked active protection due to the hydrophobicity and also to active molecule antioxidant properties. Also, it gains a high levelled impedance when compared to the original SHX formal coating that falls after 360 hrs. Oleic acid- sol-gel coating revealed an excellent resistance to post cracking after long immersion, which could open new promising applications.

Author Contributions: Conceptualisation, MM; methodology, MM, OL and NF; validation and testing MM; data analysis, MM., NF and OL; FTIR support analysis, MM, ST and DF; investigation and revalidation MM and ST; resources, MM, OL and NF; writing—original draft preparation, MM; writing—review and editing, MM, ST and NF; project supervision, NF and OL; All authors have agreed to the published this work.

Funding: This research was funded by the Libyan scholarship program as part of PhD project.

Institutional Review Board Statement: Not applicable

Informed Consent Statement: Not applicable.

Data Availability Statement: The data are not publicly available; The data files are stored on corresponding instruments and personal computers.

Acknowledgements: The authors would like to acknowledge the facilitating support by Sheffield Hallam University in Material and Engineering research institute (MERI) and also to the Libyan Scholarship Program for the financial support.

Conflicts of Interest: The authors declare no conflict of interest.

References

1. Mussa, M.H.; Rahaq, Y.; Takita, S.; Farmilo, N. Study the Enhancement on Corrosion Protection by Adding PFDTES to Hybrid Sol-Gel on AA2024-T3 Alloy in 3.5% NaCl Solutions. *Albahit J. Appl. Sci.* 2021, 2, 61–68.
2. Brinker, C.J.; Scherer, G.W. *Sol-gel science: the physics and chemistry of sol-gel processing*; George W. Scherer, C.J.B., Ed.; 1st ed.; Academic Press: New York, 1990; Vol. 3.
3. Livage, J.; Sanchez, C. *Journal of Non-Crystalline Solids.* 1992, pp. 11–19.
4. Suleiman, R.; Khaled, M.; Wang, H.; Smith, T.J.T.; Gittens, J.; Akid, R.; Ali, B.M. El; Khalil, A.; Mohamad El Ali, B.; Khalil, A. Comparison of selected inhibitor doped sol-gel coating systems for protection of mild steel. *Corros. Eng. Sci. Technol.* 2014, 49, 189–196.
5. Hamdy, A.S.; Butt, DP Environmentally compliant silica conversion coatings prepared by sol-gel method for aluminum alloys. *Surf. Coatings Technol.* 2006, 201, 401–407.
6. Tiwari, A.; Hihara, L.H.; Atul, R.; Lloyd, H.; Tiwari, A.; Hihara, L.H. Sol-Gel route for the development of smart green conversion coatings for corrosion protection of metal alloys. In *Intelligent Coatings for Corrosion Control*; Tiwari, A., Rawlins, J., Hihara, L.H., Eds.; Intelligent Coatings for Corrosion Control; Butterworth-Heinemann: Boston, 2015; pp. 363–407 ISBN 9780124114678.
7. Polmear, I.; StJohn, D.; Nie, J.-F.; Qian, M. *Physical metallurgy of aluminium alloys.* In *Light Alloys*; Butterworth-Heinemann, Elsevier Ltd: Oxford, 2017; pp. 31–107 ISBN 9780080994314.
8. Mussa, M. *Development of Hybrid Sol-Gel Coatings on AA2024-T3 with Environmentally Benign Corrosion Inhibitors*, Sheffield Hallam University, Thesis, 2020.
9. EA Frame Evaluations of preservative engine oil containing vapor-phase corrosion inhibitor and a simplified engine preservation technique. In *Interim Report BFLRF No. 269*; San Antonio, Texas, 1991; pp. 19–131.
10. National Center for Biotechnology Information. Oleic acid - PubChem - CID 445639 Available online: <https://pubchem.ncbi.nlm.nih.gov/compound/445639> (accessed on Jan 2, 2019).
11. North American Olive Oil Association What is High Oleic Oil Available online: <https://www.aboutoliveoil.org/what-is-high-oleic-oil> (accessed on Jan 2, 2019).

12. Malik, M.A.; Hashim, M.A.; Nabi, F.; Al-thabaiti, S.A. Anti-corrosion Ability of Surfactants : A Review. *Int. J. Electrochem. Sci* 2011, 6, 1927–1948. 1
13. Migahed, M.A.; Al-Sabagh, A.M. Beneficial role of surfactants as corrosion inhibitors in petroleum industry: A review article. *Chem. Eng. Commun.* 2009, 196, 1054–1075. 2
14. Zhang, W.; Guanghua, Z.; Junfeng, Z. Polyethylene glycol oleic acid based imidazoline water-soluble corrosion inhibitor and preparation method thereof 2017, 2019. 3
15. William H. Simendinger Antifouling Coating Composition 2003, 2, 1–23. 4
16. ASTM International ASTM code B209 – 14 Standard Specification for Aluminum and Aluminum-Alloy Sheet and Plate 2016, 25, 16. 5
17. Loehle, S. Understanding of adsorption mechanisms and tribological behaviors of C18 fatty acids on iron-based surfaces: a molecular simulation approach, PhD thesis. Université de Lyon, 2014. 6
18. Usoltseva, N.V.; Korobochkin, V.V.; Balmashnov, M.A.; Dolinina, A.S. Solution Transformation of the Products of AC Electrochemical Metal Oxidation. *Procedia Chem.* 2015, 15, 84–89. 7
19. Thermo scientific Knowledge base infrared spectral interpretation 2009, 1–77. 8
20. Jouet, R.J.; Warren, A.D.; Rosenberg, D.M.; Bellitto, V.J.; Park, K.; Zachariah, M.R. Surface Passivation of Bare Aluminum Nanoparticles Using Perfluoroalkyl Carboxylic Acids. *Chem. Mater.* 2005, 17, 2987–2996. 9
21. Kumar, D.; Wu, X.; Fu, Q.; Ho, JWC; Kanhere, P.D.; Li, L.; Chen, Z. Development of durable self-cleaning coatings using organic-inorganic hybrid sol-gel method. *Appl. Surf. Sci.* 2015, 344, 205–212, doi:10.1016/j.apsusc.2015.03.105. 10
22. Tait, W.S. Electrochemical impedance spectroscopy fundamentals, an introduction to electrochemical corrosion testing for practicing engineers and scientists; Tait, W.S., Ed.; PairODocs Publications: Racine, Wisconsin, USA, 1994; ISBN 13-978-0966020700. 11
23. Yabuki, A.; Yamagami, H.; Noishiki, K. Barrier and self-healing abilities of corrosion protective polymer coatings and metal powders for aluminum alloys. *Mater. Corros.* 2007, 58, 497–501. 12

13

14

15

16

17

18

19

20

21

22

23